

Tracing prices: A flow-based cost allocation for optimized power systems

F. Hofmann

October 13, 2020

Abstract

Highlights

- Flow Allocation schemes determine peer-to-peer (P2P) allocation between sources and sinks
- P2P allocation can be used to assign payments of consumers to single network assets
- Using shadow prices, Capital Expenditures are accurately allocated to users which profit from investments
- The P2P cost assignments are in alignment with the nodal pricing scheme of a welfare-maximized system
- This opens the possibility to transparently integrate transmission constraints and investment costs in national and international development plans
- Applying to a German future scenario shows how higher electricity costs arise for buses which rely on investments in transmission and local backup generation

Nomenclature

1 Introduction

Today's power systems are subject to a deep and ongoing transformation. The needed shift to from controllable to weather-driven power generation, the constant improvement and innovation of technology require rigorous system planning and international cooperation. The core of the problem manifests in the costs. Firstly, these should be as small as possible while meeting ecological and sociological standards. Secondly, they must be distributed in a fair and transparent manner. Cost-driving aspects or market

$\lambda_{n,t}$	Locational Market Price at bus n and time step t in €/MW
$d_{n,t}$	Electric demand per bus n , demand type a , time step t in MW
$g_{s,t}$	Electric generation of generator s , time step t in MW
$f_{\ell,t}$	Active power flow on line ℓ , time step t in MW
o_s	Operational price in €/MW
c_s	Capital Price in €/MW
c_ℓ	Capital Price in €/MW for transmission capacity on line ℓ
G_s	Generation capacity in MW
F_ℓ	Transmission capacity in MW
$K_{n,\ell}$	Incidence matrix

players should be detected and addressed appropriately. In this context, power system modelling has increasingly gained attention during the last years. While many studies show how cost-efficiency and renewable energy are brought together, the question of how and, more importantly, upon what grounds costs are distributed was often left open.

This study fills this gap. On the basis of an optimized network the operational state of each time step and corresponding characteristics are considered to allocate all system costs. Therefore, two basic concepts are used: Firstly, the revenue of an network asset at the cost-optimum exactly matches its operational and capital expenditures, also known as the zero-profit condition. Secondly, *flow tracing*, following Bialek's Average Participation, assigns the operation of single network assets to consumers in an plausible manner. The following shows how combining these allow for an transparent allocation of all operational (OPEX) and capital expenditures (CAPEX) to the end consumers.

2 Economic Context

In long-term operation and investment planning models, the total costs \mathcal{T} of a power system is the sum of multiple cost terms. Typically, these include OPEX for generators \mathcal{O}^G , expenditures for emissions \mathcal{E} , CAPEX for generators \mathcal{C}^G , CAPEX for the transmission system \mathcal{C}^F and so on, *i.e.*

$$\mathcal{T} = \mathcal{O}^G + \mathcal{E} + \mathcal{C}^G + \dots \quad (1)$$

In turn, each of these terms $\mathcal{C} = \{\mathcal{O}^G, \mathcal{E}, \mathcal{C}^G, \dots\}$ consists of cost associated to the asset i in the system,

$$\mathcal{C} = \sum_i \mathcal{C}_i \quad (2)$$

where an asset describes any operating part of the network, such as a generator, line, energy storage etc.

In a cost-optimal setup with minimized \mathcal{T} , the Locational Marginal Price (LMP) describes the change of costs for an incremental increase of electricity demand $d_{n,t}$ at node n and time t . Hence, it is given by the derivative of the total system cost \mathcal{T} with respect to the local demand $d_{n,t}$

$$\lambda_{n,t} = \frac{\partial \mathcal{T}}{\partial d_{n,t}} \quad (3)$$

From feeding Eq. (1) into Eq. (3) it follows natu-

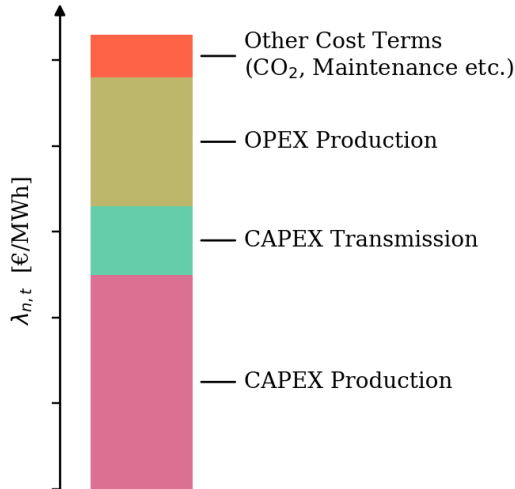


Figure 1: Schematic decomposition of the Locational Market Price $\lambda_{n,t}$. In power system model with optimal long-term operation and planning, the total system costs \mathcal{T} split into different cost terms, *i.e.* OPEX and CAPEX for production and transmission and possibly other expenditures.

rally that the LMP splits into contribution to the above mentioned cost terms. This relation, which we schematically show in Fig. 1, was already shown in extensive investigations of the LMP [13]. This leads to a nodal pricing where over the span of optimized time steps t , the system costs are partially or totally payed back by the consumers

$$\mathcal{T} - \mathcal{R} = \sum_{n,t} \lambda_{n,t} d_{n,t} \quad (4)$$

depending on the costs \mathcal{R} which are independent of the nodal demand

$$\frac{\partial \mathcal{R}}{\partial d_{n,t}} = 0 \quad (5)$$

Generally speaking, the cost term \mathcal{R} , not covered by the consumers, results from additional request to the network design, such as capacity expansion limits or minimum share of one technology in the power mix. However, in most cases, where $\mathcal{R} \ll \mathcal{T}$, these play a minor role.

However the question of how the LMP can be decomposed into contributions of single cost terms \mathcal{C}_i associated with asset i remains unanswered. This work aims at presenting and illustrating a an intuitive, peer-to-peer cost allocation including all network assets.

3 Dispatch-Based Cost Allocation

Let \mathcal{C}_i denote an arbitrary cost term associated with asset i . Consider a long-term equilibrium in a power system with perfect competition, then, according to the zero-profit condition, each cost term \mathcal{C}_i can be considered as a cost-weighted sum of the operational state $s_{i,t}$ of asset i , *i.e.*

$$\mathcal{C}_i = \sum_t \gamma_{i,t} s_{i,t} \quad (6a)$$

where $\gamma_{i,t}$ denotes a cost factor in €/MW. If \mathcal{C}_i describes the OPEX occasioned by asset i , the cost factor $\gamma_{i,t}$ is simply given by the marginal operational price o_i . However, as we will show later, if it describes the CAPEX of asset i , $\gamma_{i,t}$ is a composition of shadow prices $\mu_{i,t}$ given at the optimum.

Following the implications of Eqs. (3) and (4), we define the cost $\mathcal{C}_{n \rightarrow i,t}$ that consumers at bus n have pay to asset i at time t , in order to compensate for

\mathcal{C}_i , as

$$\mathcal{C}_{n \rightarrow i, t} = \gamma_{i, t} \frac{\partial s_{i, t}}{\partial d_{n, t}} d_{n, t} \quad (6b)$$

The derivative on the right hand side is defined through the sensitivity of the operational variable $s_{i, t}$ at the optimum against changes in the demand. However, we replace this quantity by

$$\frac{\partial s_{i, t}}{\partial d_{n, t}} d_{n, t} \Leftrightarrow A_{i, n, t} \quad (6c)$$

where $A_{i, n, t}$ represents the amount of power that asset i supplies demand $d_{n, t}$ with. As we will show later, it is calculated from established flow allocation schemes. By following this approach, the differential quantity on the left side, is replaced by an integral quantity. The latter does not only rely on a marginal sensitivity of the nodal demand $d_{n, t}$, but makes further assumptions on how the operational state $s_{i, t}$, all in all, serves consumers in the network. The dispatch allocation $A_{i, n, t}$ ensures that all power produced or processed by asset i at time t is assigned to consumers,

$$s_{i, t} = \sum_n A_{i, n, t}, \quad (6d)$$

from which follows that the sum of all cost contributions return the total cost term,

$$\mathcal{C}_i = \sum_{n, t} \mathcal{C}_{n \rightarrow i, t} \quad (6e)$$

By combining Eqs. (6b) and (6c), we are able to formulate a full cost allocation from demand to network assets for every time-step t . In particular, the definition of cost factors $\gamma_{i, t}$ must be derived for each cost term individually. In the following we depict the presented scheme for typical classes of assets. Therefore, we assume a network with generators s , transmission lines ℓ and storage units r , each asset $i = \{s, \ell, r\}$ adds a term for OPEX and a term for CAPEX to the total system cost \mathcal{T} .

3.1 OPEX Allocation

Let the operational price for an asset i be given by o_i . Then, the OPEX occasioned, for example, by generator s is given by

$$\mathcal{O}_s^G = \sum_t o_s g_{s, t} \quad (7)$$

where $g_{s, t}$ denotes its power generation at time t . Equation (7) matches the form of Eq. (6a) which allows us to use the above presented scheme in Eqs. (6). As a result we obtain

$$\mathcal{O}_{n \rightarrow s, t} = o_s A_{s, n, t} \quad (8)$$

which is the contribution of $d_{n, t}$ to the OPEX at generator s . The quantity

$$A_{s, n, t} \Leftrightarrow \frac{\partial g_{s, t}}{\partial d_{n, t}} d_{n, t} \quad (9)$$

superseding the derivative on the right side, describes the power that is produced by generator s and consumed at node n at time t .

In the same manner, we can follow the scheme to allocate OPEX for flow $f_{\ell, t}$ and storage unit dispatch $g_{r, t}^{\text{dis}}$. As we assume a bidirectional flow on line ℓ , the OPEX is set proportional to the absolute value of the flow. The upper section in Table 1 shows the mapping of variables to Eqs. (6) in order to define the full OPEX allocation.

The scheme works for all other cost attached to the operational state of an asset i . Given for example a fix price for emissions μ_{CO_2} in € per tonne- CO_2 equivalents, the cost term for emission adds up to

$$\mathcal{E} = \mu_{\text{CO}_2} \sum_s e_s g_{s, t} \quad (10)$$

where e_s denotes the emission factor in tonne- CO_2 per MWh_{el} of generator s . The allocated payment for consumers at bus n at time t assigned to generator s is then given by

$$\mathcal{E}_{n \rightarrow s, t} = \mu_{\text{CO}_2} e_s A_{s, n, t} \quad (11)$$

3.2 CAPEX Allocation

For the CAPEX allocation, it becomes crucial to look at the individual relations between operational state $s_{i, t}$ and its binding constraints. For all assets, let the capital price for one MW capacity expansion be denoted by c_i . All quantities for the CAPEX allocation, which we now discuss in detail, are summarized in the lower section of Table 1.

3.2.1 Generators

The nominal capacity G_s constrains the generation $g_{s, t}$ in the form of

$$g_{s, t} - \bar{g}_{s, t} G_s \leq 0 \perp \bar{\mu}_{s, t} \quad \forall s, t \quad (12)$$

$$-g_{s, t} \leq 0 \perp \underline{\mu}_{s, t} \quad \forall s, t \quad (13)$$

	i	\mathcal{C}	\mathcal{C}_i	$\gamma_{i,t}$	$s_{i,t}$
OPEX Production	s	\mathcal{O}^G	$\sum_t o_s g_{s,t}$	o_s	$g_{s,t}$
OPEX Transmission	ℓ	\mathcal{O}^F	$\sum_t o_\ell f_{\ell,t} $	o_ℓ	$ f_{\ell,t} $
OPEX Storage	r	\mathcal{O}^E	$\sum_t o_r g_{r,t}^{\text{dis}}$	o_r	$g_{r,t}$
Emission Cost	s	\mathcal{E}	$\mu\text{CO}_2 e_s g_{s,t}$	$\mu\text{CO}_2 e_s$	$g_{s,t}$
CAPEX Production	s	\mathcal{C}^G	$c_s G_s$	$\bar{\mu}_{s,t}$	$g_{s,t}$
CAPEX Transmission	ℓ	\mathcal{C}^F	$c_\ell F_\ell$	$(\bar{\mu}_{\ell,t} - \underline{\mu}_{\ell,t})$	$f_{\ell,t}$
CAPEX Storage	r	\mathcal{C}^E	$c_r G_r$	$\bar{\mu}_{r,t}^{\text{dis}} - \underline{\mu}_{r,t}^{\text{dis}} + (\eta_r^{\text{dis}})^{-1} \lambda_{r,t}^{\text{ene}}$	$g_{r,t}$

Table 1: Mapping of different cost terms to the cost allocation scheme given in Eqs. (6). These include OPEX & CAPEX for production, transmission and storage assets in the network, as well as a cost term for the total Green House Gas (GHG) emissions.

where $\bar{g}_{s,t} \in [0, 1]$ is the capacity factor for renewable generators. At a cost-optimum, these two constraints yield the shadow prices $\bar{\mu}_{s,t}$ and $\underline{\mu}_{s,t}$. As shown in [3] and in detailed in Appendix A.3, over the whole time span, the CAPEX for generator s is paid back by the production $g_{s,t}$ times the shadow price $\bar{\mu}_{s,t}$,

$$\mathcal{C}_s^G = c_s G_s = \sum_t \bar{\mu}_{s,t} g_{s,t} \quad (14)$$

This representation connects the CAPEX with the operational state of generator s , *i.e.* matches the form in Eq. (6a). The resulting the CAPEX allocation is given by

$$\mathcal{C}_{n \rightarrow s,t}^G = \bar{\mu}_{s,t} A_{s,n,t} \quad (15)$$

How does this allocation behave? According to the polluter pays principle, it differentiates between consumers who are ‘responsible’ for investments and those who are not. If $\bar{\mu}_{s,t}$ (in literature often denoted as the Quality of Supply) is bigger than zero, the upper Capacity Constr. (12) is binding, which pushes investments in G_s . If $\bar{\mu}_{s,t} = 0$, the generation $g_{s,t}$ is not bound and investments are not necessary. When summing over all CAPEX payments to generator s in Eq. (15), we can use Eqs. (6d) and (14) to see that each generator retrieves exactly the cost that were spent to build the capacity G_s .

3.2.2 Transmission Lines

The transmission capacity F_ℓ limits the flow $f_{\ell,t}$ in both directions,

$$f_{\ell,t} - F_\ell \leq 0 \perp \bar{\mu}_{\ell,t} \quad \forall \ell, t \quad (16)$$

$$-f_{\ell,t} - F_\ell \leq 0 \perp \underline{\mu}_{\ell,t} \quad \forall \ell, t \quad (17)$$

which yield the shadow prices $\bar{\mu}_{\ell,t}$ and $\underline{\mu}_{\ell,t}$. Again, we use the result of [3] (for details see Appendix A.4) which shows that over the whole time span, the investment in line ℓ is paid back by the shadow prices times the flow

$$\mathcal{C}_\ell^F = c_\ell F_\ell = \sum_t (\bar{\mu}_{\ell,t} - \underline{\mu}_{\ell,t}) f_{\ell,t} \quad (18)$$

From here, we follow the scheme in Eqs. (6) which finally defines the CAPEX allocation as

$$\mathcal{C}_{n \rightarrow \ell,t}^F = (\bar{\mu}_{\ell,t} - \underline{\mu}_{\ell,t}) A_{\ell,n,t} \quad (19)$$

The quantity

$$A_{\ell,n,t} \Leftrightarrow \frac{\partial f_{\ell,t}}{\partial d_{n,t}} d_{n,t} \quad (20)$$

represents the flow that the demand at node n and time t causes on line ℓ . The shadow prices $\bar{\mu}_{\ell,t}$ and $\underline{\mu}_{\ell,t}$ again can be seen as a measure for necessity of transmission investments at ℓ at time t . Hence, the definition of $\mathcal{C}_{n \rightarrow \ell,t}^F$ states that consumers, which retrieve power flowing on congested lines, yielding a bound Constr. (16) or (17), pay compensations for the resulting investments at ℓ . Again the sum of all CAPEX payments to line ℓ equals the total CAPEX spent. This is seen when summing Eq. (19) over all buses and time steps and using Eqs. (6d) and (18)

3.2.3 Storages

In a simplified storage model, G_r limits the storage dispatch $g_{r,t}^{\text{dis}}$ and charging $g_{r,t}^{\text{sto}}$. Further it limits the maximal storage capacity $g_{r,t}^{\text{ene}}$ by a fix ratio h_r , denoting the maximum hours at full discharge. The storage r dispatches power with efficiency η_r^{dis} , charges power with efficiency η_r^{sto} and

preserves power from one time step t to the next, $t + 1$, with an efficiency of η_r^{ene} . In Appendix A.5 we formulate the mathematical details. As already shown in [3], the total expenditures at r are fully paid back by differences of the LMP at which the storage “buys” and “sells” power. Taking only the CAPEX into account the zero profit condition reduces to

$$\begin{aligned} \mathcal{C}^E &= c_r G_r \\ &= \sum_t \left(\bar{\mu}_{r,t}^{\text{dis}} - \underline{\mu}_{r,t}^{\text{dis}} + (\eta_r^{\text{dis}})^{-1} \lambda_{r,t}^{\text{ene}} \right) g_{r,t}^{\text{dis}} \\ &\quad - \sum_t \lambda_{n,t} K_{n,r} g_{r,t}^{\text{sto}} \quad \forall r \end{aligned} \quad (21)$$

where $\bar{\mu}_{r,t}^{\text{dis}}$ and $\underline{\mu}_{r,t}^{\text{dis}}$ are the shadow prices of the upper and lower dispatch capacity bound and $\lambda_{r,t}^{\text{ene}}$ is the shadow price of the energy balance constraint. When applying the cost allocation scheme Eqs. (6), it stands to reason to assume that $\partial g_{r,t}^{\text{sto}} / \partial d_{n,t} \cdot d_{n,t} \Leftrightarrow 0$, implying that the when a storage charges power, it does not supply any demand. At these times, it the storage is a effective consumer retrieving power from producing assets. This leaves us with

$$\mathcal{C}_{n \rightarrow r,t}^E = \left(\bar{\mu}_{r,t}^{\text{dis}} - \underline{\mu}_{r,t}^{\text{dis}} + (\eta_r^{\text{dis}})^{-1} \lambda_{r,t}^{\text{ene}} \right) A_{r,n,t} \quad (22)$$

where the dispatch allocation only assigns discharge power to demand $d_{n,t}$, thus

$$A_{r,n,t} \Leftrightarrow \frac{\partial g_{r,t}^{\text{dis}}}{\partial d_{n,t}} d_{n,t} \quad (23)$$

Note that this relation will break Eq. (6e) as the payments to r surpass the CAPEX by an amount \mathcal{R}_r^E . It is crucial to note that storage units perform a redistribution of money, and therefore distort the cost allocation. So, a certain share of what is allocated to the CAPEX of a storage is in another time step spent by the same storage in order to buy power from other assets. This effect scales with the amount of installed storage capacity.

We shortly annotate that it is possible to incorporate this redistribution into the cost allocation, by replacing the demand $d_{n,t}$ with the power charge $g_{r,t}^{\text{sto}}$ in Eqs. (6). Then, the derived payments that a storage unit r has to pay to asset i is given by $\mathcal{C}_{r \rightarrow i}$. The sum of those payments due to r will the sum up to \mathcal{R}_r^E .

3.3 Design Constraints

Power system modelling does rarely follow a pure Greenfield approach with unlimited capacity expansion.

Rather, today’s models are setting various constraints defining socio-political or technical requirements. As mentioned before this will alter the equality of total cost and total revenue, *i.e.* leads to $\mathcal{R} \neq 0$ in Eq. (4). More precisely, each constraint h_j (other than the nodal balance constraint) of the form

$$h_j(s_{i,t}, S_i) - K < 0 \quad (24)$$

where K is any non-zero constant and S_i is collects all capacities of asset i , will result in a cost term contributing to \mathcal{R} and alter Eq. (6a) to

$$\mathcal{C}_i - \mathcal{R}_i = \sum_t \gamma_{i,t} s_{i,t} \quad (25)$$

The total allocatable cost associated to cost term \mathcal{C} is then given by

$$\mathcal{C}' = \sum_i \mathcal{C}_i - \mathcal{R}_i \quad (26)$$

According to the nature of Eq. (24) and the corresponding \mathcal{R}_i , it is either larger, equal or lower than \mathcal{C} . In the following we highlight two often used classes of designs constraints in the form of Eq. (24) and show how to incorporate them into the cost allocation.

3.3.1 Capacity Expansion Limit

In more realistic setups, generators, lines or other assets can only be built up to a certain limit. This might be due to land use restrictions or social acceptance problems. However, when constraining the capacity S_i for a subset I of assets to an upper limit \bar{S} , in the form of

$$S_i - \bar{S} \leq 0 \quad \perp \quad \bar{\mu}_i^{\text{nom}} \quad \forall i \in I, \quad (27)$$

the zero profit condition alters as soon as the constraint becomes binding. Then, the revenue of asset i exceeds its total expenditures (OPEX + CAPEX). More precisely, the allocated CAPEX in Table 1 will surpass the actual CAPEX of asset i by the cost it has to pay for the scarcity, given by the absolute value of

$$\mathcal{R}_i^{\text{scarcity}} = -\bar{\mu}_i^{\text{nom}} S_i \quad \forall i \in I \quad (28)$$

The share of the CAPEX allocation, which results from the scarcity, is given by

$$\mathcal{R}_{n \rightarrow i,t}^{\text{scarcity}} = \frac{\bar{\mu}_i^{\text{nom}}}{c_i + \bar{\mu}_i^{\text{nom}}} \mathcal{C}_{n \rightarrow i,t}^I \quad \forall i \in I \quad (29)$$

where $\mathcal{C}_{n \rightarrow i,t}^I$ denotes the CAPEX allocation presented above.

3.3.2 Brownfield Constraints

In order to take already built infrastructure into account, the capacity S_i can be constrained to a minimum required capacity \underline{S} . Mathematically this translates to

$$\underline{S} - S_i \leq 0 \quad \perp \quad \mu_i^{\text{nom}} \quad \forall i \in I \quad (30)$$

Again, such a setup alters the zero profit condition of asset i , as soon as the constraint becomes binding. In that case, asset i does not collect enough revenue in order to match the CAPEX. The difference, given by

$$\mathcal{R}_i^{\text{subsidy}} = \mu_i^{\text{nom}} S_i \quad \forall i \quad (31)$$

has to be subsidized by governments or communities. It is rather futile wanting to allocate these cost to consumers as assets may not gain any revenue for their operational state, *i.e.* where $\mathcal{C}^I = \mathcal{R}_i^{\text{subsidy}}$.

4 Assumptions on Power Allocations

The presented cost allocation suits for any type of topology and network setup. It may be extended by other classes of network assets or design constraints. But so far, the question of how the allocation $A_{i,n,t}$ for generators s , lines ℓ and storages r are defined was left open.

In a first step, we show that the needed information narrows down to peer-to-peer allocations between producing assets and consumers. Let $p_{m,t}$ denote the net power injection at node m and time t . It is given by

$$p_{m,t} = \sum_{i \in \{s,r\}} K_{m,i} s_{i,t} - d_{m,t} \quad (32)$$

where $K_{m,i}$ is 1 if asset i is attached to bus m and zero otherwise. Now, let $H_{\ell,n}$ denote a linear mapping between the injection $p_{m,t}$ and the flow $f_{\ell,t}$, such that

$$f_{\ell,t} = \sum_m H_{\ell,m} p_{m,t} \quad (33)$$

Usually, $H_{\ell,n}$ is given by the Power Transfer Distribution Factors (PTDF) which indicate the changes in the flow on line ℓ for one unit (typically one MW) of net power production at bus m . For transport models or mixed AC-DC networks, these can be calculated or extended using the formulation presented in [9].

Using the two expressions the derivative of the flow $f_{\ell,t}$ with respect to the demand can be expressed through

$$\frac{\partial f_{\ell,t}}{\partial d_{n,t}} d_{n,t} \Leftrightarrow A_{\ell,n,t} = \sum_m H_{\ell,m} (A_{m \rightarrow n,t} - \delta_{n,m} d_{n,t}), \quad (34)$$

where we collected all power produced at bus m and consumed at bus n in $A_{m \rightarrow n,t}$, defined as

$$A_{m \rightarrow n,t} = \sum_{i \in \{S,R\}} K_{m,i} A_{i,n,t} \quad (35)$$

Equation (34) shows that $A_{\ell,n,t}$ is fully determined through the peer-to-peer allocation $A_{m \rightarrow n,t}$. In other words, we only need to know how much of the power produced at node m is consumed at node n . With this information we may also derive the cost allocation for the transmission system. Unfortunately, the solution for $A_{m \rightarrow n,t}$ is non-unique and requires further assumptions. Established flow allocation schemes approach this problem from different directions. Principally two options exist *what* is allocated

1. gross power injections
2. net power injections

Further it is important *what assumptions* define the allocation, *i.e.* what method is used to define the pairs of sources and sinks. The three suitable approaches we present here are

- a. Equivalent Bilateral Exchanges (EBE) [7] which assumes that every producer supplies every consumer proportional to its share in the total consumption.
- b. Average Participation (AP) [2, 1] which traces the flow from producer to consumer following the law of proportional sharing.
- c. Flow Based Market Coupling (FBMC) which uses zonal PTDF for allocating power within predefined regions. The interregional exchange is only allocating net power deficit or excess of the regions.

We show the mathematical formulation for all combinations **a1** - **c2** in Appendices B.1 to B.4. Principally, allocating net power instead of gross power leads to less P2P trades, as power from a bus m with $g_{m,t} \leq d_{m,t}$ is not assigned to other buses, only to m .

When it comes to the methods, as literature has often pointed out, the EBE principal does not suit for large networks where remote buses would interconnect in the same way as buses in close vicinity [8]. The AP allocation tackles this problem by restricting P2P trades to those which are traceable when applying the proportional sharing principal. Therefore $A_{s,n,t}$ denotes that part of power produced by bus m which, when following in the direction of $f_{\ell,t}$, ends up at bus n . In contrast, the FBMC allows to control the regions or market zones which are netted out in a first step. If in a region R the generation undercuts the demand, $\sum_{n \in R} g_{n,t} \leq \sum_{n \in R} d_{n,t}$, none of the inner-regional generation is assigned to other regions. However, it relies on further assumptions such as the Generation Shift Keys determining the producing assets which are deployed for the inter-regional exchange.

From this point of view, we restrict the focus of this research to **net** injection allocation on the basis of **AP**, type **2b**, as locality and no further dependency on external decisions are strong arguments for a transparent cost allocation. We emphasize that the AP based allocation does not imply traceability of the resulting flows, as it only determines the *source-sink* relations $A_{m \rightarrow n,t}$. The flow allocation still follows the power flow equation given as shown in Eq. (34). In the following example, we illustrate the functionality of the cost allocation by an example of a small artificial network.

4.1 Numerical Example

Consider a two bus system, depicted in Fig. 2, with one transmission line and one generator per bus. Generator 1 (at bus 1) has a cheap operational price of 50 €/MWh_{el}, generator 2 (at bus 2) has a expensive operational price of 200 €/MWh_{el}. For both, capital investments amount 500 €/MW and the maximal capacity is limited to $\bar{G}_s = 100$ MW. The transmission line has a capital price of 100 €/MW and no upper capacity limit. With a demand of 60 MW at bus 1 and 90 MW at bus 2, the optimization expands the cheaper generator at bus 1 to its full limit of 100 MW. The 40 MW excess power, not consumed at bus 1, flows to bus 2 where the generator is built with only 50 MW.

Figure 3 shows the allocated transactions on the basis of allocation **2b** for both buses 1 & 2 separately. Note, the “sum” of the two figures give to the actual

dispatch. The resulting P2P payments are given in Fig. 4.

The left graph Fig. 3a shows that d_1 is with 60 MW totally supplied by the local production. Consequently consumers at bus 1 pay 3k € OPEX, which is the operational price of 50 € times the 60 MW. Further they pay 33k € for the CAPEX at generator 1. Note that 3k € of these account for the scarcity imposed buy the upper expansion limit \bar{G}_s . The rest makes up 60% of the total CAPEX spent at generator 1, exactly the share of power allocated to d_1 . Consumers at bus 1 don’t pay any transmission CAPEX as no flow is associated with there demand. The right graph Fig. 3b shows the power allocations to d_2 . We see that 50 MW are self-supplied whereas the remaining 40 MW are imported from bus 1. Thus, consumers have the pay for the local OPEX and CAPEX as well as the proportional share of expenditures at bus 1 and the transmission system. As the capacity at generator 2 does not hit the expansion limit \bar{G}_s , no scarcity cost are assigned to it. The allocated CAPEX $C_{2 \rightarrow 2,t}^G$ compensates the actual CAPEX of generator 2. Again, in the case of generator 1, 2k € of the 22k € CAPEX allocation are associated with the scarcity cost for generator 1. The payed congestion revenue of 4k € is exactly the CAPEX of the transmission line, which directly reflects the zero-profit condition. The sum of all values in the payoff matrix in Fig. 4 yield $\mathcal{T} - \mathcal{R}^{\text{scarcity}}$, the total system cost minus the scarcity cost (which in turn is negative). The sum of a column yields the total revenue per the asset i . These values match their overall spending plus the cost of scarcity. The sum a row returns the total payment of consumers at bus n . For example the sum of payments of consumers at bus 1 is 36k €. This is exactly the electricity price of 600 €/MW times the consumption of 60 MW, $\lambda_1 d_1$.

The fact that OPEX and CAPEX allocations are proportional to each other results from optimizing one time step only. This coherence breaks for larger optimization problems with multiple time steps. Then CAPEX allocation takes effect only for time steps in which one or more of the capacity constraints Constrs. (12), (16) and (17) become binding.

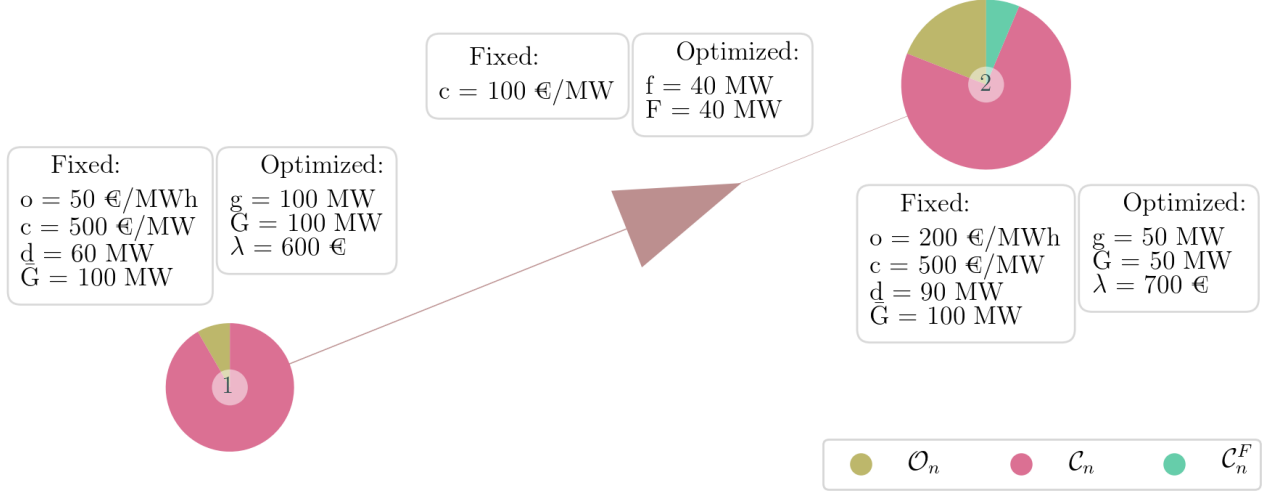


Figure 2: Illustrative example of a 2-bus network with one optimized time step. Fixed prices and constraining values are given in the left box for each bus and the transmission line. Optimized values are given in the right boxes. Bus 1 has a cheaper operational price o , capital prices are the same for both. As both generator capacities are constraint to 100 MW, the optimization also deploys the generator at bus 2. The resulting electricity prices λ are then a composition of all prices for operation and capital investments.

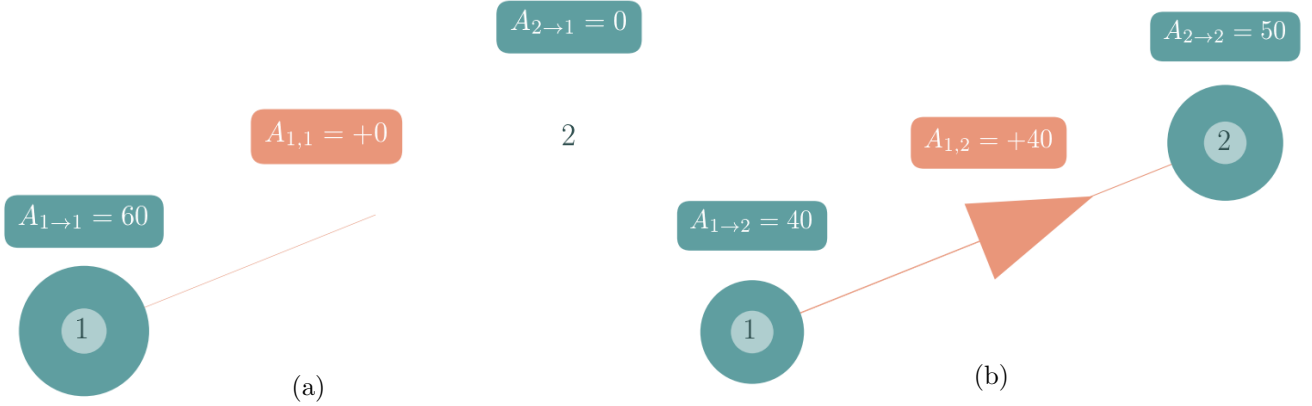


Figure 3: Power allocations of net power injections using the AP scheme, type 2b, in the example network, Fig. 2. Consumers at for bus 1, figure (a), are, with 60 MW, totally supplied by the local generator and do not consume any imported power from bus 2. In contrast consumer at bus 2, figure (b), retrieve 40 MW from generator 1, induce a flow of 40 MW on the transmission line and consume 50 MW from the local generator.

5 Application Case

We showcase the behavior of the cost allocation in a more complex system, by applying it to an cost-optimized German power system model with 50 nodes and one year time span with hourly resolution. The model builds up on the PyPSA-EUR workflow [11] with technical details and assumptions reported in [10].

We follow a brownfield approach where transmission lines can be expanded starting from today's capacity values, originally retrieved from the ENTSO-E Transmission System Map [6]. Pre-installed wind and solar generation capacity totals of the year 2017 were distributed in proportion to the average power potential at each site excluding those with an average capacity factor of 10%. Further, wind and solar capacity expansion are limited by land use re-

		\mathcal{O}		\mathcal{C}^G		\mathcal{C}^F
n	1	3k €	0k €	33k €	0k €	0k €
	2	2k €	10k €	22k €	25k €	4k €
		1	2	1	2	1
		s		s		ℓ

Figure 4: Full P2P cost allocation on the basis of power allocations shown in Fig. 3. Consumers compensate OPEX and CAPEX of the generators they retrieve from, see Fig. 3. As bus 1 is totally self-supplying, all its payment is assigned to the local generator. As bus 2 imports power from bus 1 and thus induces a flow on line 1, it not only compensates local expenditures but also OPEX and CAPEX at bus 1 and CAPEX for the transmission.

striction. These consider agriculture, urban, forested and protected areas based on the CORINE and NATURA2000 database [4, 5]. Pumped Hydro Storages (PHS) and Run-of-River power plants are fixed to today’s capacities with no more expansion allowed. Additionally, unlimited expansion of batteries and H₂-storages and Open-Cycle Gas Turbines (OCGT) are allowed at each node. We impose an effective carbon price of 120 € per tonne-CO₂ which, for OCGT, adds an effective price of 55 €/MWh_{el} (assuming a gross emission of 180 kg/MWh and an efficiency of 39%). All cost assumptions on operational costs o_i and annualized capital cost c_i are summarized in detail in Table 2.

The optimized network is shown in Fig. 5. On the left we find the lower capacity bounds for renewable generators and transmission infrastructure, on the right the capacity expansion for generation, storage and transmission are displayed. The optimization expands solar capacities in the south, onshore and offshore wind in the upper north and most west. Open-Cycle Gas Turbines (OCGT) are built within the broad middle of the network. Transmission lines are amplified along the North-South axis, including one large DC link, associated with the German Süd-Link, leading from the coastal region to the South-West. The total annualized cost of the power system roughly sums up to 42 billion €.

Figure 6 displays the average electricity price $\lambda_{n,t}$

per region. We observe a relatively strong gradient from south (at roughly 92 €/MWh) to north (80 €/MWh). Regions with little pre-installed capacity and capacity expansion, especially for renewables, tend to have higher prices. The node with the lowest LMP in the upper North-West, stands out through high pre-installed offshore capacities.

The costs are allocated according to type 2b. For allocating flows on DC-lines we use the method described in [9]. In Fig. 7 we show the total of all “allocatable” costs \mathcal{C}' . Due to the design constraints, Section 3.3, and storage units, Section 3.2.3, these are different from the original cost terms \mathcal{C} . The figure also includes costs for scarcity $\mathcal{R}^{\text{scarcity}}$ and subsidy $\mathcal{R}^{\text{subsidy}}$. Note that the sum of all contributions in Fig. 7 equals the total cost \mathcal{T} .

The largest proportion of the payments is associated with CAPEX for generators, transmission system and storage units in decreasing order. Taking different technologies into account, we observe a fundamental difference between the controllable OCGT and the variable renewable resources: As shown in detail in Fig. C.6, more than half of all investments in OCGT is determined in one specific hour. At this time (morning, end of February), the system hits the highest mismatch between low renewable power potential and high demand. The necessity for backup generators manifests in high allocation of CAPEX and consequently high LMP. With a few exceptions in the South West and East, all consumers receive power from OCGT at this time, thus all pay high amounts for the needed backup infrastructure (operational state of the system is in detailed shown in Fig. C.7). Note that this is the most extreme event, which ensures backup infrastructure for other inferior extreme events. The total CAPEX allocation for OCGT infrastructure is depicted in Fig. C.1d. This correlates with our findings of the extreme event.

Contrary to this, CAPEX for renewable infrastructure are allocated evenly throughout several thousands of hours. As for onshore and offshore wind farms, the produced power deeply penetrates the network, see Fig. C.4, thus it is not only local, but also remote consumers which cover the CAPEX, see Fig. C.1. This in turn benefits local consumers, which profit from the cheap power which explains why these regions end up with a low average LMP.

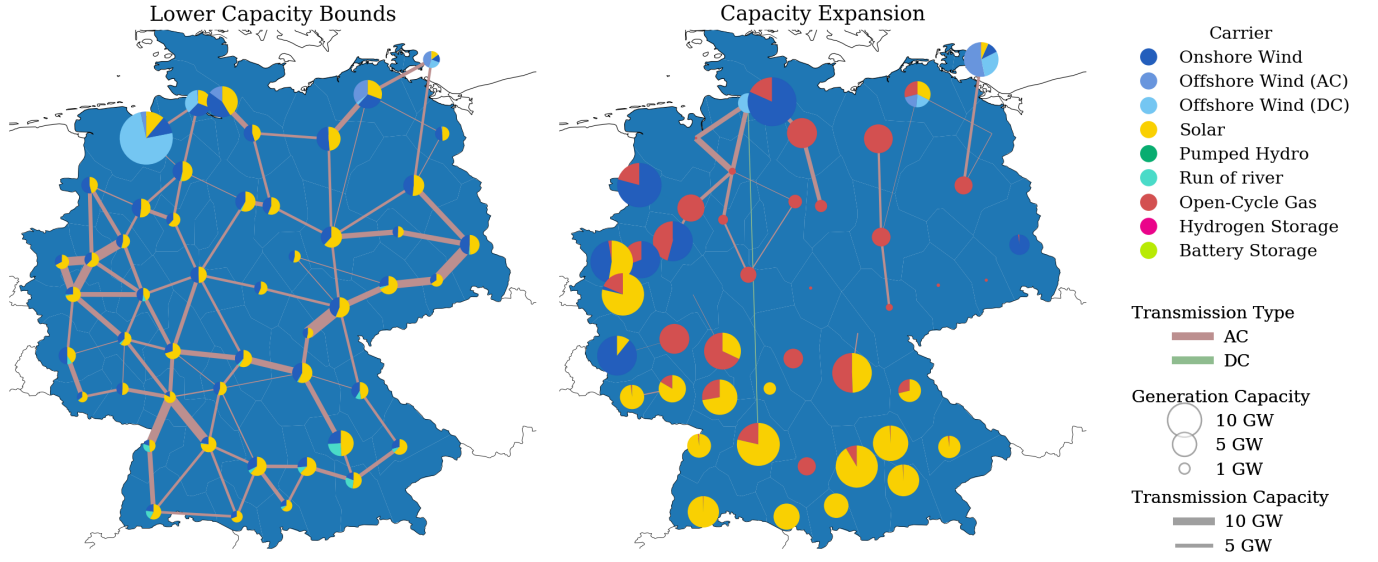


Figure 5: Brownfield optimization of the German power system. The left side shows existent renewable capacities, matching the total capacity for the year 2017, which serve as lower capacity limits for the optimization. The right side shows the capacity expansion of renewables as well as installation of backup power plants. The effective CO₂ price is set to 120 €/per tonne CO₂ emission.

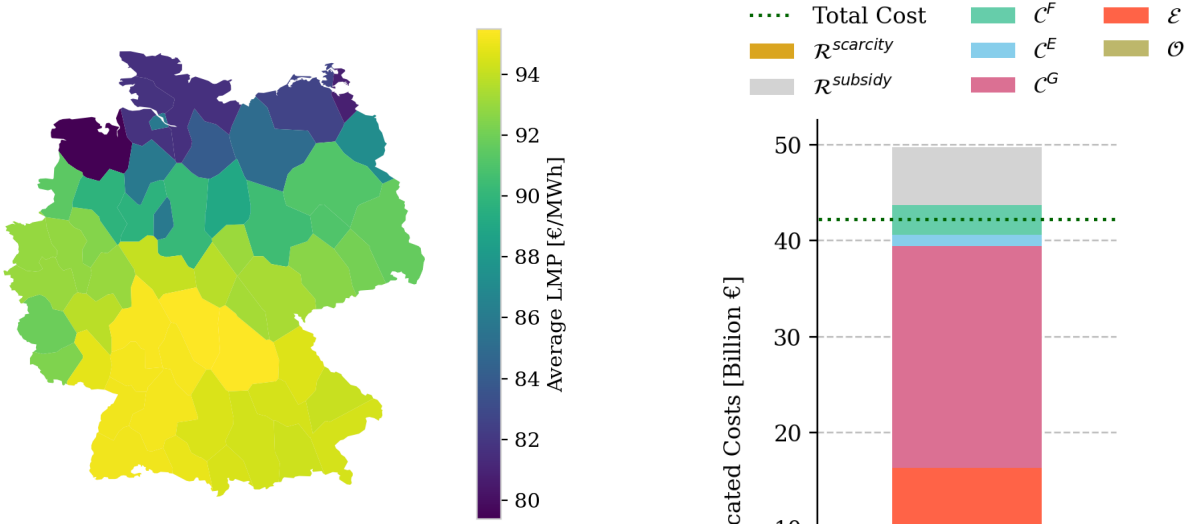


Figure 6: Average electricity price $\langle \lambda_{n,t} \rangle_t$ per region as a result from the optimization of the German power system. Regions in the middle and south of Germany have high prices whereas electricity in the North with a strong wind, transmission and OCGT infrastructure is cheaper.

Figure 7: Total allocated payments of the system.

Together with the emission cost \mathcal{E} , the total OPEX \mathcal{O} amount around 16 billion €. As to expect, 99.97% are dedicated to OCGT alone, as these have by far the highest operational price. For a detailed regional distribution of payments per MWh and the resulting revenues for generator, see Figs. C.2 and C.3. For OCGT, the spatial allocation of the OPEX clearly differs from the CAPEX allocation. This results from the fact that during ordinary demand peaks, it is rather local OCGT generators which serve as backup generators. In the average power mix per region, see Fig. C.4, we observe that regions with strong OCGT capacities predominately have high shares of OCGT power. The OPEX allocations for renewables play with 0.2 €/MWh in average an inferior role.

The negative segment in Fig. 7 is associated with scarcity costs $\mathcal{R}^{\text{scarcity}}$, caused by land use constraints for renewables and the transmission expansion limit. These sum up approximately to 7.5 b€. Note again, that according to Eq. (28) this term is negative and is part of the allocated CAPEX payments. It translates to the cost that consumers pay “too much” for assets limited in their capacity expansion. In the real world this money would be spent for augmented land costs or civic participation in the dedicated areas. In Fig. C.9 we give a detailed insight of how the scarcity cost manifest in the average cost per consumed MWh. The scarcity for wind and solar is relatively low and impact the average price at roughly 2€/MWh. It primarily affects, different to the pure CAPEX allocation, regions in close vicinity. Remarkably, the scarcity cost per MWh for run-of-river power plants amounts up to 16€. This high impact is due to the steady power potential from run-off water and the strong limitation of capacity expansion. However, as these power plants in particular are already amortized, the scarcity cost should be reconsidered and removed from a final cost allocation.

A high influence on the price comes from the scarcity of transmission expansion. Right beside regions with high wind infrastructure, it occasions costs higher than MWh 4€/MWh (maximal 8€/MWh), see Fig. C.8. As to expect, the constraint mainly suppresses transmission expansion along the north-south axis.

The last cost term in Fig. 7, is caused by lower capacity constraints for pre-existing assets. These violate the optimal design and are not compen-

sated through the nodal payments $d_{n,t} \lambda_{n,t}$. Most of these “non-allocatable” costs account for Pumped Hydro Storage, onshore wind, offshore wind and the transmission system, see Fig. C.5 for further details. Again, as most of the named assets are already amortized (PHS, transmission system), the subsidy should be reconsidered in a final cost allocation.

In Fig. 8 we compare the total cost allocation of the region with the lowest average LMP (left side) against the one of the region with the highest LMP (right side). The region with the cheapest electricity is in the Northwest. We see that this bus is fairly independent of investments in the transmission system, as it is supplied by steady, cheap offshore power. Moreover, the CAPEX of the local offshore wind farms are partly paid by subsidies, see Fig. C.5. Only a small share of the payments is allocated to remote OCGTs, resulting from the extreme event mentioned earlier.

In contrast the regions with the highest LMP, spends most its money to local OCGT operations, emission cost and the transmission system. Its payments to onshore and offshore wind infrastructure are low despite a third of its supply comes from wind power. Instead, a lot of its payments are assigned to the transmission infrastructure. Hence, the wind power supply at this region is not restricted by exhausted wind power resources but by bottlenecks in the transmission system.

6 Conclusion

In this work we presented a new cost-allocation scheme based on peer-to-peer dispatch allocations from asset to consumer. Starting from an optimized long-term investment model, we were able to decompose single cost terms into contributions of single consumers. For three typical classes of assets, namely generators, transmission lines and storage units, we showed how operational prices and shadow prices must be weighted with the dispatch allocation in order to allocate all system costs. Further we highlighted the impact of additional design constraints, that is constraints with a non-zero constant on the right hand side, such as lower and upper capacity expansion limits. These alter the locational marginal price and therefore distort the cost allocations. In the case of upper capacity expansion limits, this leads to an additional charge for consumers which have to compensate for *e.g.* land use restrictions. For lower

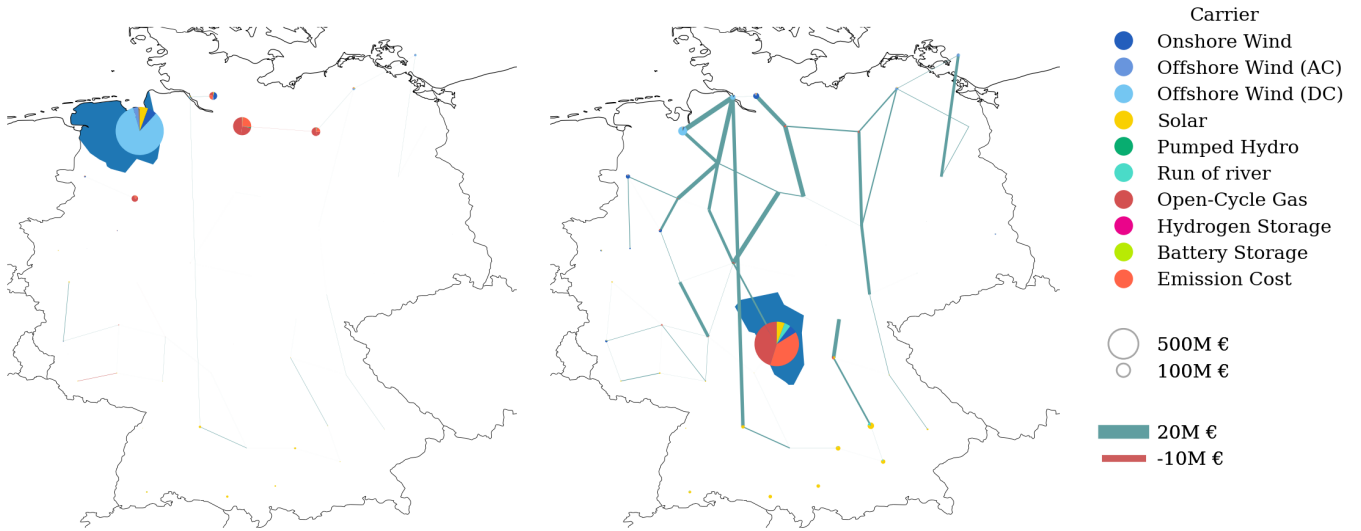


Figure 8: Comparison of payments of the node with the **lowest LMP (left)** and the node with the **highest LMP (right)**. The region of the paying bus is colored in dark blue. The circles indicate where to which bus and technology combined OPEX and CAPEX payments. Further the thickness of the lines indicates the dedicated amount of payments. The cheap prices in the North...

capacity investment bounds, the cost have to be subsidized by the overall system operator or the government, as those cannot be allocated. ...

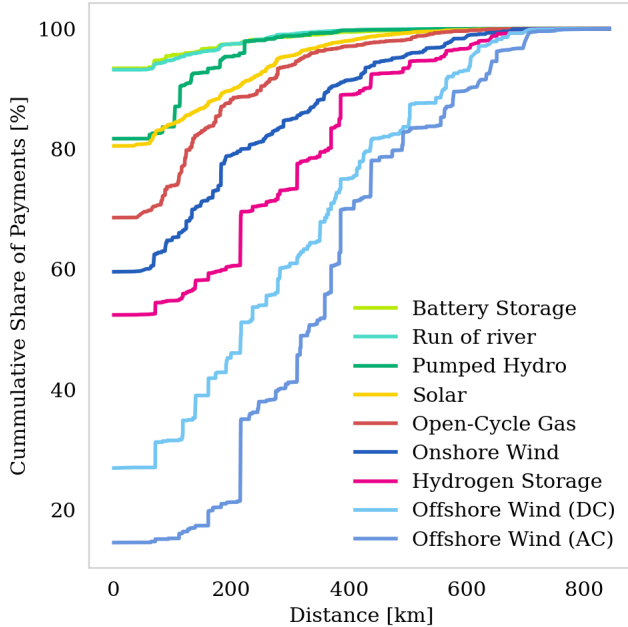


Figure 9: Average distance between payer and receiver for different technologies and shares of the total production.

A Network Optimization

A.1 LMP from Optimization

The nodal balance constraint ensures that the amount of power that flows into a bus equals the power that flows out of a bus, thus reflects the Kirchhoff Current Law (KCL). Alternatively, we can the demand $d_{n,t}$ has to be supplied by the attached as-sets,

$$\sum_i K_{n,i} s_{i,t} = d_{n,t} \perp \lambda_{n,t} \quad \forall n, t \quad (\text{A.1})$$

where $K_{n,i}$ is +1 if i is attached to n and a positive operation $s_{i,t}$ delivers power to n , -1 if is attached to n and a positive operation retrieves power from n and zero else (note that for lines this results in the negative of the conventional Incidence Matrix). The shadow price of the nodal balance constraint mirrors the Locational Marginal Prizes (LMP) $\lambda_{n,t}$ per bus and time step. In a power market this is the €/MWh_{el}-price which a consumer has to pay.

A.2 Full Lagrangian

The Lagrangian for the investment model can be condensed to the following expression

$$\begin{aligned} \mathcal{L}(s_{i,t}, S_i, \lambda_{n,t}, \mu_j) = & \sum_{i,t} o_i s_{i,t} + \sum_i c_i S_i \\ & + \sum_{n,t} \lambda_{n,t} \left(d_{n,t} - \sum_i K_{n,i} s_{i,t} \right) \\ & + \sum_j \mu_j h_j(s_{i,t}, S_i) \end{aligned} \quad (\text{A.2})$$

where $h_j(s_{i,t}, S_i)$ denotes all inequality constraints attached to $s_{i,t}$ and S_i . In order to impose the Kirchhoff Voltage Law (KVL) for the linearized AC flow, the term

$$\sum_{\ell,c,t} \lambda_{c,t} C_{\ell,c} x_\ell f_{\ell,t} \quad (\text{A.3})$$

can be added to \mathcal{L} , with x_ℓ denoting the line's impedance and $C_{\ell,c}$ being 1 if ℓ is part of the cycle c and zero otherwise.

The global maximum of the Lagrangian requires stationarity with respect to all variables:

$$\frac{\partial \mathcal{L}}{\partial s_{i,t}} = \frac{\partial \mathcal{L}}{\partial S_i} = 0 \quad (\text{A.4})$$

A.3 Zero Profit Generation

Constrs. (12) and (13), which yield the KKT variables $\bar{\mu}_{s,t}$ and $\underline{\mu}_{s,t}$, imply the complementary slackness,

$$\bar{\mu}_{s,t} (g_{s,t} - \bar{g}_{s,t} G_s) = 0 \quad \forall n, s, t \quad (\text{A.5})$$

$$\underline{\mu}_{s,t} g_{s,t} = 0 \quad \forall n, s, t \quad (\text{A.6})$$

The stationarity of the generation capacity variable leads to

$$\frac{\partial \mathcal{L}}{\partial G_s} = 0 \rightarrow c_s = \sum_t \bar{\mu}_{s,t} \bar{g}_{s,t} \quad \forall n, s \quad (\text{A.7})$$

and the stationarity of the generation to

$$\frac{\partial \mathcal{L}}{\partial g_{s,t}} = 0 \rightarrow o_s = K_{n,s} \lambda_{n,t} - \bar{\mu}_{s,t} + \underline{\mu}_{s,t} \quad \forall n, s \quad (\text{A.8})$$

Multiplying both sides of Eq. (A.7) with G_s and using Eq. (A.5) leads to

$$c_s G_s = \sum_t \bar{\mu}_{s,t} g_{s,t} \quad (\text{A.9})$$

The zero-profit rule for generators is obtained by multiplying Eq. (A.8) with $g_{s,t}$ and using Eqs. (A.6) and (A.9) which results in

$$c_s G_s + \sum_t o_s g_{s,t} = \sum_t \lambda_{n,t} K_{n,s} g_{s,t} \quad (\text{A.10})$$

It states that over the whole time span, all OPEX and CAPEX for generator s (left hand side) are payed back by its revenue (right hand side).

A.4 Zero Profit Transmission System

The yielding KKT variables $\bar{\mu}_{\ell,t}$ and $\underline{\mu}_{\ell,t}$ are only non-zero if $f_{\ell,t}$ is limited by the transmission capacity in positive or negative direction, i.e. Constr. (16) or Constr. (17) are binding. For flows below the thermal limit, the complementary slackness

$$\bar{\mu}_{\ell,t} (f_{\ell,t} - F_\ell) = 0 \quad \forall \ell, t \quad (\text{A.11})$$

$$\underline{\mu}_{\ell,t} (f_{\ell,t} - F_\ell) = 0 \quad \forall \ell, t \quad (\text{A.12})$$

sets the respective KKT to zero.

The stationarity of the transmission capacity to

$$\frac{\partial \mathcal{L}}{\partial F_\ell} = 0 \rightarrow c_\ell = \sum_t (\bar{\mu}_{\ell,t} - \underline{\mu}_{\ell,t}) \quad \forall \ell \quad (\text{A.13})$$

and the stationarity with respect to the flow to

$$0 = \frac{\partial \mathcal{L}}{\partial f_{\ell,t}} \quad (\text{A.14})$$

$$0 = - \sum_n K_{n,\ell} \lambda_{n,t} + \lambda_{c,t} C_{\ell,c} x_{\ell} - \bar{\mu}_{\ell,t} + \underline{\mu}_{\ell,t} \quad \forall n, s \quad (\text{A.15})$$

When multiplying Eq. (A.13) with F_{ℓ} and using the complementary slackness Eqs. (A.11) and (A.12) we obtain

$$c_{\ell} F_{\ell} = \sum_t (\bar{\mu}_{\ell,t} - \underline{\mu}_{\ell,t}) f_{\ell,t} \quad (\text{A.16})$$

Again we can use this to formulate the zero-profit rule for transmission lines. We multiply Eq. (A.15) with $f_{\ell,t}$, which finally leads us to

$$c_{\ell} F_{\ell} = - \sum_n K_{n,\ell} \lambda_{n,t} f_{\ell,t} + \lambda_{c,t} C_{\ell,c} x_{\ell} f_{\ell,t} \quad (\text{A.17})$$

It states that the congestion revenue of a line (first term right hand side) reduced by the cost for cycle constraint exactly matches its CAPEX.

A.5 Zero Profit Storage Units

For an simplified storage model, the upper capacity G_r limits the discharging dispatch $g_{r,t}^{\text{dis}}$, the storing power $g_{r,t}^{\text{sto}}$ and state of charge $g_{r,t}^{\text{ene}}$ of a storage unit r by

$$g_{r,t}^{\text{dis}} - G_r \leq 0 \quad \forall r, t \perp \bar{\mu}_{r,t}^{\text{dis}} \quad (\text{A.18})$$

$$g_{r,t}^{\text{sto}} - G_r \leq 0 \quad \forall r, t \perp \bar{\mu}_{r,t}^{\text{sto}} \quad (\text{A.19})$$

$$g_{r,t}^{\text{ene}} - h_r G_r \leq 0 \quad \forall r, t \perp \bar{\mu}_{r,t}^{\text{ene}} \quad (\text{A.20})$$

where we assume a fixed ratio between dispatch and storage capacity of h_r . The state of charge must be consistent throughout every time step according to what is dispatched and stored,

$$g_{r,t}^{\text{ene}} - \eta_r^{\text{ene}} g_{r,t-1}^{\text{ene}} - \eta_r^{\text{sto}} g_{r,t}^{\text{sto}} + (\eta_r^{\text{dis}})^{-1} g_{r,t}^{\text{dis}} = 0 \quad \perp \lambda_{r,t}^{\text{ene}} \quad \forall r, t \quad (\text{A.21})$$

We use the result of Appendix B.3 in [3] which shows that a storage recovers its capital (and operational) costs from aligning dispatch and charging to the LMP, thus

$$\sum_t o_r g_{r,t}^{\text{dis}} + c_r G_r = \sum_t \lambda_{n,t} K_{n,r} (g_{r,t}^{\text{dis}} - g_{r,t}^{\text{sto}}) \quad (\text{A.22})$$

The stationarity of the dispatched power leads us to

$$\frac{\partial \mathcal{L}}{\partial g_{r,t}^{\text{dis}}} = 0 \quad o_r - \lambda_{n,t} K_{n,r} - \underline{\mu}_{r,t}^{\text{dis}} + \bar{\mu}_{r,t}^{\text{dis}} + (\eta_r^{\text{dis}})^{-1} \lambda_{r,t}^{\text{ene}} = 0 \quad (\text{A.23})$$

which we can use to define the revenue which compensates the CAPEX at r ,

$$c_r G_r = \sum_t \left(\bar{\mu}_{r,t}^{\text{dis}} - \underline{\mu}_{r,t}^{\text{dis}} + (\eta_r^{\text{dis}})^{-1} \lambda_{r,t}^{\text{ene}} \right) g_{r,t}^{\text{dis}} - \sum_t \lambda_{n,t} K_{n,r} g_{r,t}^{\text{sto}} \quad \forall r \quad (\text{A.24})$$

A.6 Emission Constraint

Imposing an additional CO₂ constraint limiting the total emission to K ,

$$\sum_{n,s,t} e_s g_{s,t} \leq K \perp \mu_{\text{CO}_2} \quad (\text{A.25})$$

with e_s being the emission factor in tonne-CO₂ per MWh_{el}, returns an effective CO₂ price μ_{CO_2} in €/tonne-CO₂. As shown in ... the constraint can be translated in a dual price which shift the operational price per generator

$$o_s \rightarrow o_s + e_s \mu_{\text{CO}_2} \quad (\text{A.26})$$

B Allocation Schemes

B.1 Allocating Gross Injections with EBE

The allocation of gross generation to demands $d_{n,t}$ is straightforwardly obtained by a proportional distribution of the generation, *i.e.*

$$A_{s,n,t} = \frac{g_{s,t}}{\sum_s g_{s,t}} d_{n,t} \quad (\text{B.27})$$

B.2 Allocating Net Injections with EBE

Allocating net power injections using the EBE methods leads to the same result as the Marginal Participation (MP) [12] algorithm when allocating to consumers only, see [9] for further insight. We calculate it by setting

$$A_{m \rightarrow n,t} = \delta_{m,n} p_{m,t}^{\circ} + \gamma_t p_{n,t}^{-} p_{m,t}^{+} \quad (\text{B.28})$$

where

- $p_{n,t}^+ = \min(g_{n,t} - d_{n,t}, 0)$ denotes the nodal net production
- $p_{n,t}^- = \min(d_{n,t} - g_{n,t}, 0)$ denotes the nodal net consumption
- $p_{n,t}^\circ = \min(p_{n,t}^+, p_{n,t}^-)$ the denotes nodal self-consumption. That is the power generated and at the same time consumed at node n and
- $\gamma_t = (\sum_n p_{n,t}^+)^{-1} = (\sum_n p_{n,t}^-)^{-1}$ is the inverse of the total injected/extracted power at time t .

The allocation $A_{s,n,t}$ from generator s to n , is given by multiplying $A_{m \rightarrow n,t}$ with the nodal share $g_{s,t}/g_{n,t}$.

B.3 Allocating Net Power using AP

Allocating net injections using the AP method is derived from [1]. In a lossless network the downstream and upstream formulations result in the same P2P allocation which is why we restrict ourselves to the downstream formulation only. In a first step we define a time-dependent auxiliary matrix \mathcal{J}_t which is the inverse of the $N \times N$ with directed power flow $m \rightarrow n$ at entry (m, n) for $m \neq n$ and the total flow passing node m at entry (m, m) at time step t . Mathematically this translates to

$$\mathcal{J}_t = (\text{diag}(p^+) + \mathcal{K}^- \text{diag}(f) K)_t^{-1} \quad (\text{B.29})$$

where \mathcal{K}^- is the negative part of the directed Incidence matrix $\mathcal{K}_{n,\ell} = \text{sign}(f_{\ell,t}) K_{n,\ell}$. Then the distributed slack for time step t is given by

$$A_{m \rightarrow n,t} = \mathcal{J}_{m,n,t} p_{m,t}^+ p_{n,t}^- \quad (\text{B.30})$$

B.4 Allocating Gross Power using AP

We use the same allocation as in Appendix B.3 but replace the net nodal production $p_{n,t}^+$ by the gross nodal production $g_{n,t}$ which leads to

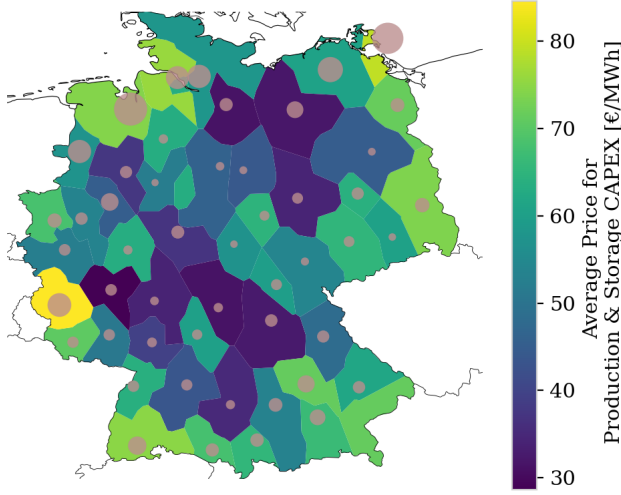
$$\mathcal{J}_t = (\text{diag}(g) + \mathcal{K}^- \text{diag}(f) K)_t^{-1} \quad (\text{B.31})$$

The distributed slack is for time step t is then given by

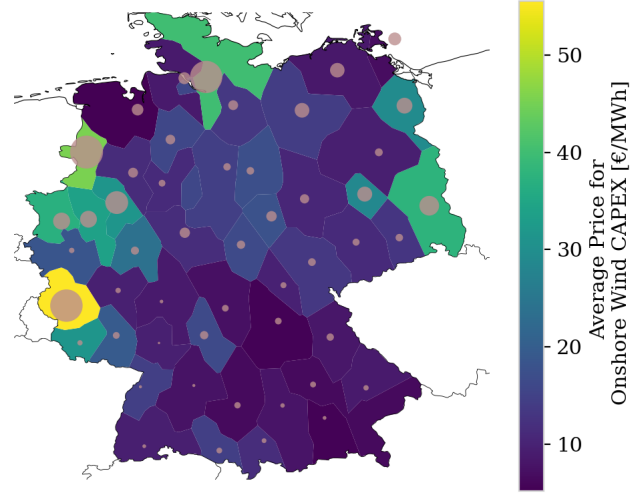
$$A_{s \rightarrow m,t} = \mathcal{J}_{m,n} g_{s,t} d_{n,t} \quad (\text{B.32})$$

C Working Example

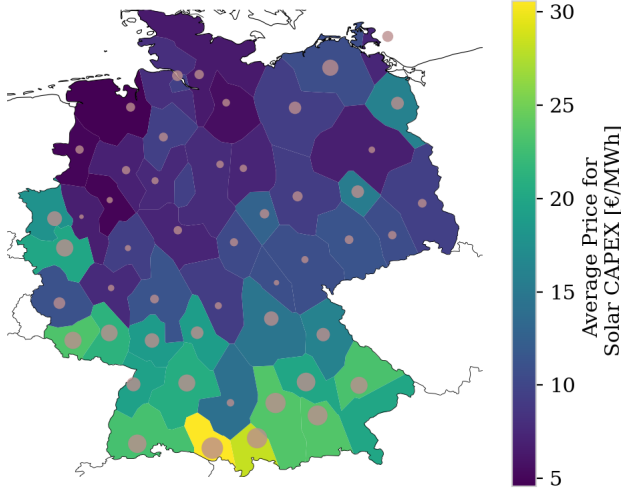
The following figures contain more detailed information about the peer-to-peer cost allocation. The cost or prices paid by consumers are indicated by the region color. The dedicated revenue is displayed in proportion to the size of cycles (for assets attached to buses) or to the thickness of transmission branches.



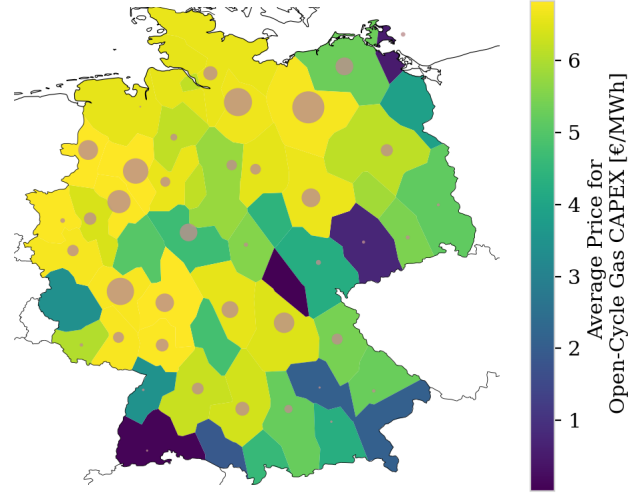
(a) All production and storage technologies



(b) Onshore Wind



(c) Solar



(d) OCGT

Figure C.1: Average **CAPEX allocation** per MWh, $\sum_t c_{n \rightarrow s,t}^G / \sum_t d_{n,t}$ and $\sum_t c_{n \rightarrow r,t}^E / \sum_t d_{n,t}$, for all production and storage assets (a), onshore wind (b), solar (c) and OCGT (d). Average Allocated CAPEX per MWh within the regions are indicated by the color, the revenue per production asset is given by the size of the circles at the corresponding bus.

		o [€/MWh]	c [k€/MW]*
carrier			
Generator	Open-Cycle Gas	120.718	47.235
	Offshore Wind (AC)	0.015	204.689
	Offshore Wind (DC)	0.015	230.532
	Onshore Wind	0.015	109.296
	Run of river		270.941
	Solar	0.01	55.064
Storage	Hydrogen Storage		224.739
	Pumped Hydro		160.627
	Battery Storage		133.775
Line	AC		0.038
	DC		0.070

Table 2: Operational and capital price assumptions for all type of assets used in the working example. The capital price for transmission lines are given in [k€/MW/km]. The cost assumptions are retrieved from the PyPSA-EUR model [11].

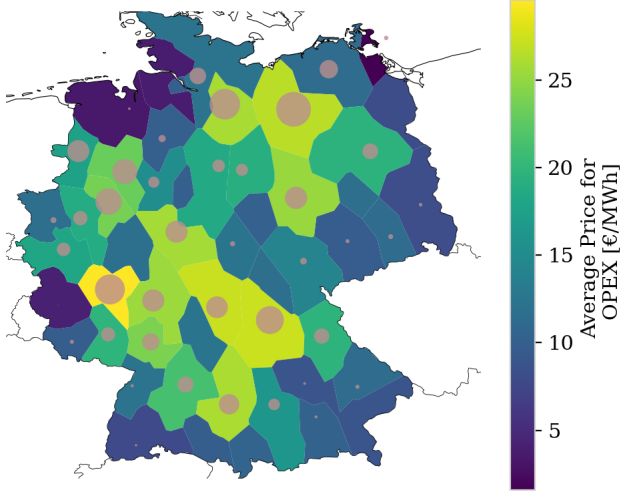


Figure C.2: Average **OPEX allocation** per consumed MWh, $\sum_t \mathcal{O}_{n \rightarrow s, t} / \sum_t d_{n, t}$. The effective prices for OPEX are indicated by the color of the region, the size of the circles are set proportional to the revenue per regional generators and storages. As OCGT is the only allowed fossil based technology, the drawn allocation is proportional to OPEX allocation of OCGT generators.

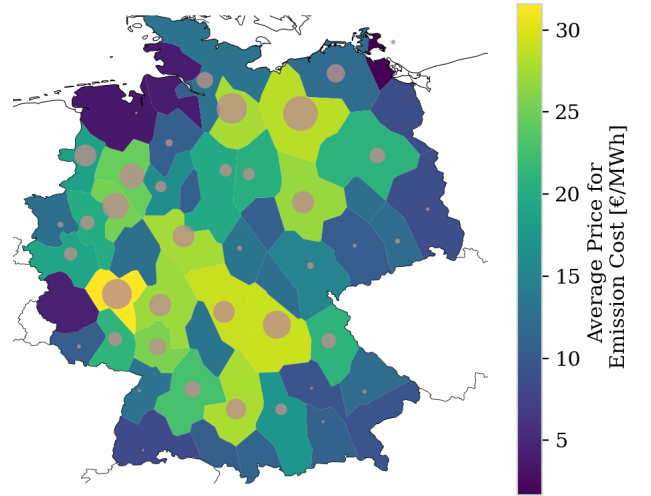


Figure C.3: Average **allocated emission cost**, $\sum_t \mathcal{E}_{n \rightarrow s, t}$, per consumed MWh. The effective prices are indicated by the color of the region, the size of the circles are set proportional to the revenue per regional generators.

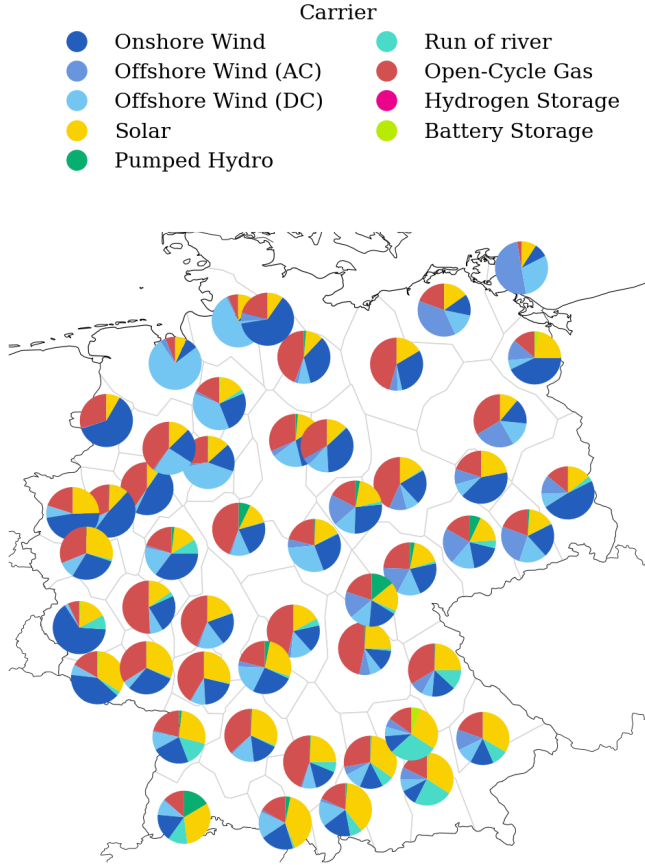


Figure C.4: Average power mix per region calculated by Average Participation **b**. Coastal regions are mainly supplied by local offshore and onshore wind farms. Their strong power injections additionally penetrate the network up to the southern border. In the middle and South, the supply is dominated by a combination of OCGT and solar power.

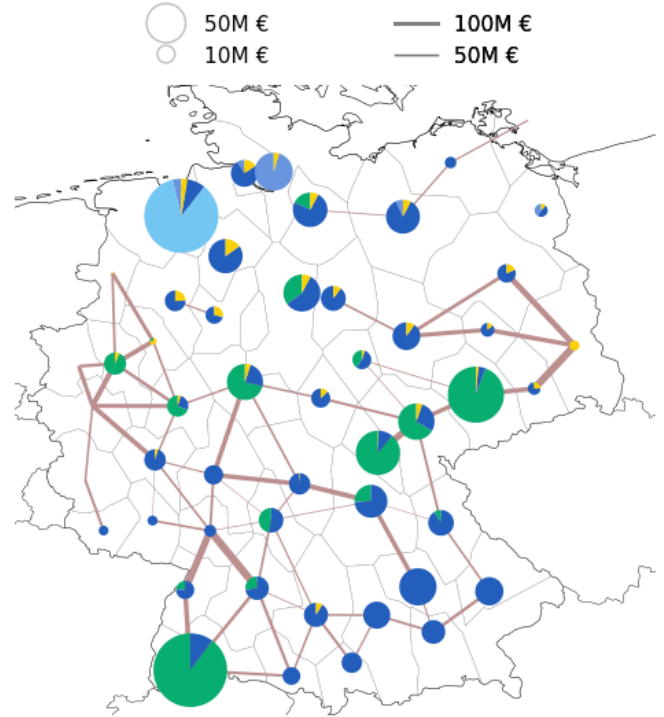


Figure C.5: Total costs for subsidy $\mathcal{R}^{\text{subsidy}}$ resulting from lower capacity expansion bounds (brown-field constraints). The figure shows the built infrastructure that does not gain back its CAPEX from its market revenue, but is only build due to lower capacity limits.

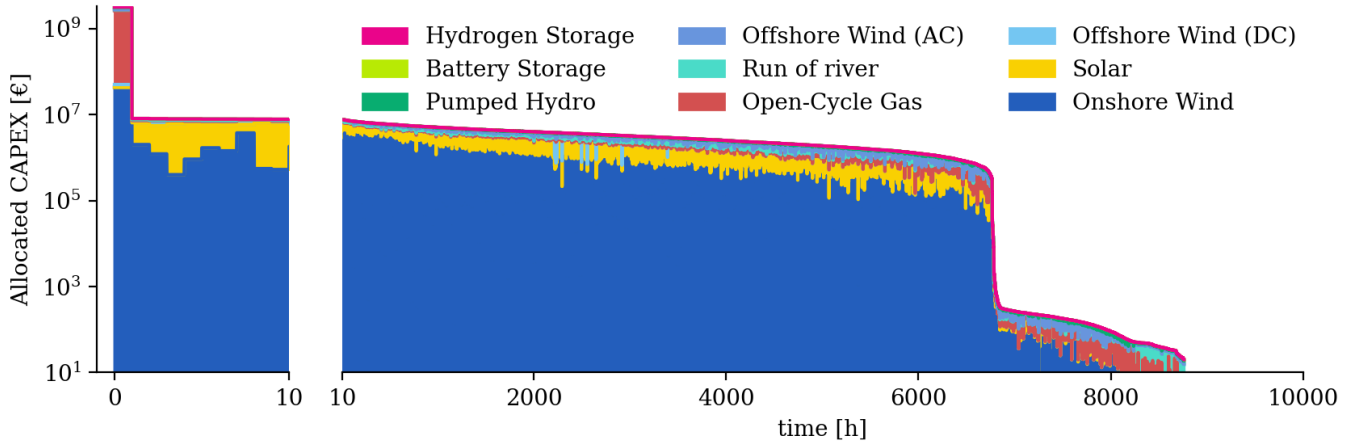


Figure C.6: Duration curve of the CAPEX allocation for production and storage technologies. Hours are sorted by the total amount of allocated expenditure. With 2.7 bn € the first value pushes investments extraordinarily high. Due to low renewable potentials, it is dominated by CAPEX for OCGT which receives 92% of the payments. This hour alone occasions about the half of all OCGT CAPEX. Figure C.6 gives a detailed picture of the operational state at this time-step. The following 7000 time-steps are dominated by revenues for onshore wind and reveal a rather even distribution. In hours of low CAPEX allocation (after the second drop) spendings for OCGT start to increase again. These time-steps however play a minor role.

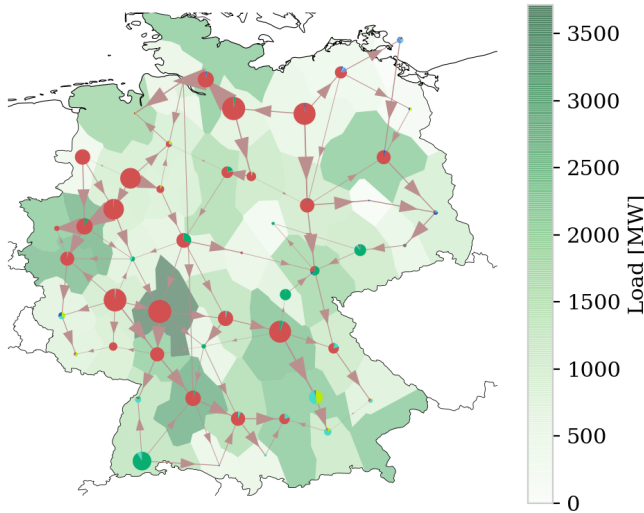


Figure C.7: Production, flow and consumption in the system at the hour with the highest allocated expenditures. The size of the circles are proportional to the power production at a node. Size of arrows are proportional to the flow on the transmission line. The depicted hour corresponds to the first value in the duration curve in Fig. C.6.

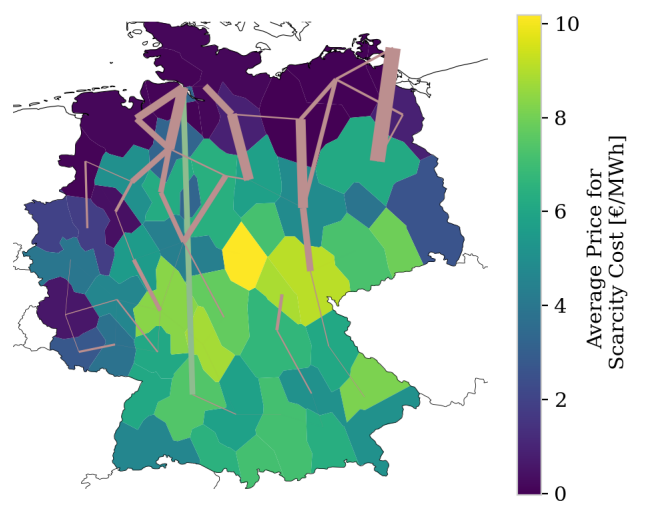
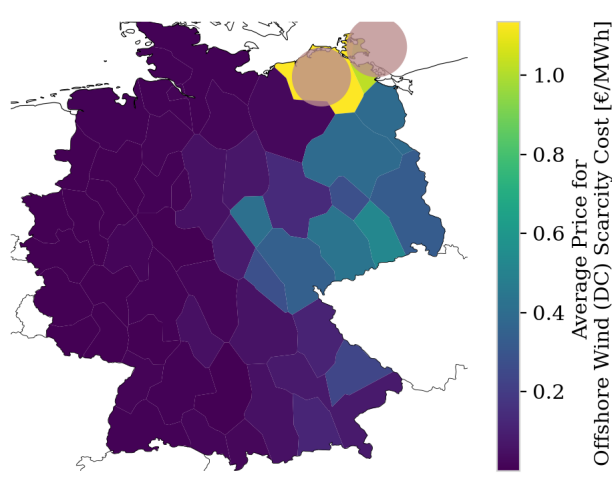
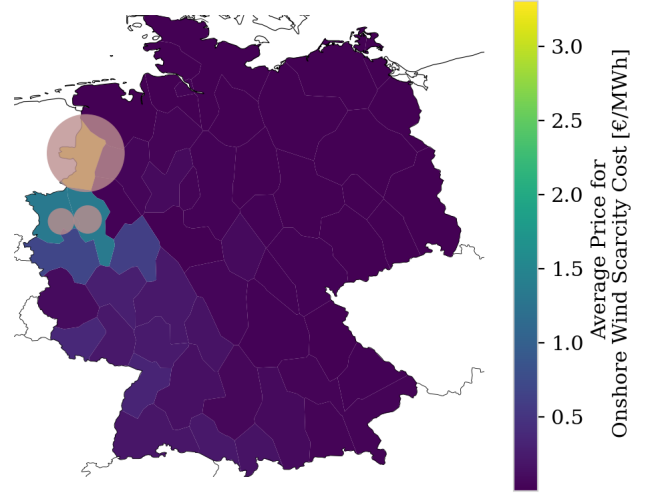


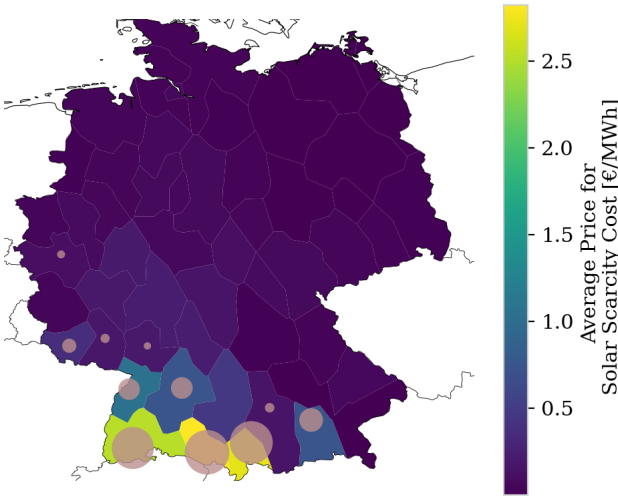
Figure C.8: Average **allocated transmission scarcity cost** per consumed MWh, $\sum_t \mathcal{R}_{n \rightarrow \ell, t}^{\text{scarcity}} / \sum_t d_{n, t}$. This scarcity cost results from the upper transmission expansion limit of 25%. The costs are indicated by the regional color. The lines are drawn in proportion to revenue dedicated to scarcity cost.



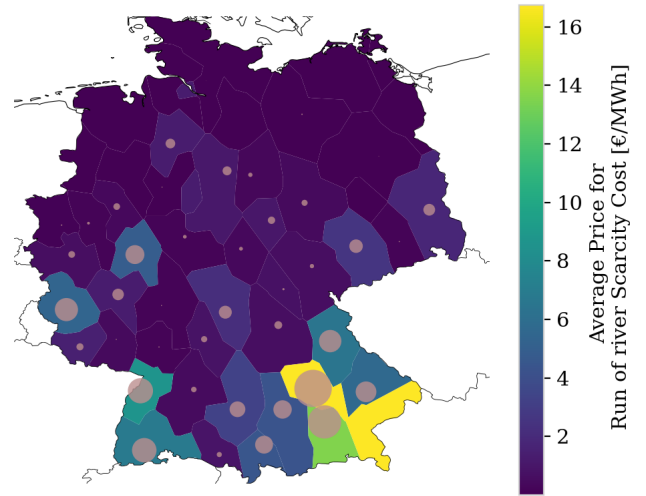
(a) Offshore Wind



(b) Onshore Wind



(c) Solar



(d) Run-of-River

Figure C.9: Average **allocated scarcity cost** per consumed MWh, $\sum_t \mathcal{R}_{n \rightarrow i, t}^{\text{scarcity}} / \sum_t d_{n, t}$. These cost result from land use restrictions for offshore wind, onshore wind, solar, run-of-river. The cost per MWh are indicated by the color of a region. The revenue per production asset is given by the size of the circle at the corresponding bus.

References

- [1] Chira Achayuthakan et al. “Electricity Tracing in Systems With and Without Circulating Flows: Physical Insights and Mathematical Proofs”. en. In: *IEEE Transactions on Power Systems* 25.2 (May 2010), pp. 1078–1087. ISSN: 0885-8950, 1558-0679. DOI: [10.1109/TPWRS.2009.2037506](https://doi.org/10.1109/TPWRS.2009.2037506).
- [2] J. Bialek. “Tracing the Flow of Electricity”. en. In: *IEE Proceedings - Generation, Transmission and Distribution* 143.4 (1996), p. 313. ISSN: 13502360. DOI: [10.1049/ip-gtd:19960461](https://doi.org/10.1049/ip-gtd:19960461).
- [3] T. Brown and L. Reichenberg. “Decreasing Market Value of Variable Renewables Is a Result of Policy, Not Variability”. In: *arXiv:2002.05209 [econ, math, q-fin]* (Feb. 2020). arXiv: [2002.05209 \[econ, math, q-fin\]](https://arxiv.org/abs/2002.05209).
- [4] EEA. “Corine Land Cover (CLC) 2012, Version 18.5.1”. In: (2012).
- [5] EEA. “Natura 2000 Data - the European Network of Protected Sites”. In: (2016).
- [6] ENTSO-E. *ENTSO-E Transmission System Map*. en-us. <https://www.entsoe.eu/data/map/>.
- [7] F.D. Galiana, A.J. Conejo, and H.A. Gil. “Transmission Network Cost Allocation Based on Equivalent Bilateral Exchanges”. en. In: *IEEE Transactions on Power Systems* 18.4 (Nov. 2003), pp. 1425–1431. ISSN: 0885-8950. DOI: [10.1109/TPWRS.2003.818689](https://doi.org/10.1109/TPWRS.2003.818689).
- [8] H.A. Gil, F.D. Galiana, and A.J. Conejo. “Multi-area Transmission Network Cost Allocation”. en. In: *IEEE Transactions on Power Systems* 20.3 (Aug. 2005), pp. 1293–1301. ISSN: 0885-8950. DOI: [10.1109/TPWRS.2005.851951](https://doi.org/10.1109/TPWRS.2005.851951).
- [9] Fabian Hofmann et al. “Flow Allocation in Meshed AC-DC Electricity Grids”. en. In: *Energies* 13.5 (Mar. 2020), p. 1233. ISSN: 1996-1073. DOI: [10.3390/en13051233](https://doi.org/10.3390/en13051233).
- [10] Jonas Hörsch et al. “PyPSA-Eur: An Open Optimisation Model of the European Transmission System”. English. In: *Energy Strategy Reviews* 22 (Nov. 2018), pp. 207–215. ISSN: 2211467X. DOI: [10.1016/j.esr.2018.08.012](https://doi.org/10.1016/j.esr.2018.08.012).
- [11] Jonas Hörsch et al. *PyPSA-Eur: An Open Optimisation Model of the European Transmission System (Code)*. Zenodo. June 2020. DOI: [10.5281/ZENODO.3520874](https://doi.org/10.5281/ZENODO.3520874).
- [12] H. Rudnick, R. Palma, and J.E. Fernandez. “Marginal Pricing and Supplement Cost Allocation in Transmission Open Access”. In: *IEEE Transactions on Power Systems* 10.2 (May 1995), pp. 1125–1132. ISSN: 08858950. DOI: [10.1109/59.387960](https://doi.org/10.1109/59.387960).
- [13] Fred C. Schweppe et al. *Spot Pricing of Electricity*. en. Boston, MA: Springer US, 1988. ISBN: 978-1-4612-8950-0 978-1-4613-1683-1. DOI: [10.1007/978-1-4613-1683-1](https://doi.org/10.1007/978-1-4613-1683-1).